

Substituted Heterocyclic Naphthalene Diimides with Unexpected Acidity. Synthesis, Properties, and Reactivity

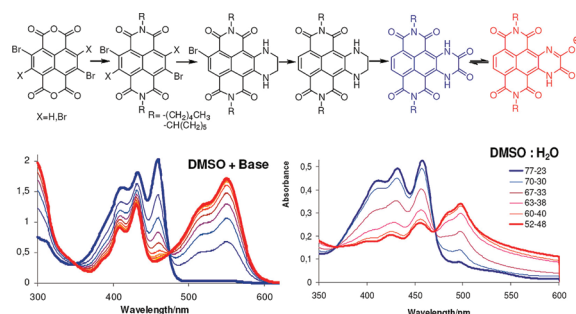
Filippo Doria,[†] Marco di Antonio,[‡] Michele Benotti,[†] Daniela Verga,[†] and Mauro Freccero^{*†}

[†]Dipartimento di Chimica Organica, Università di Pavia, V. le Taramelli 10, 27100 Pavia, Italy, and

[‡]Dipartimento di Scienze Farmaceutiche, Università di Padova, Via Marzolo, 5, 35131 Padova, Italy

mauro.freccero@unipv.it

Received August 10, 2009



Naphthalene bisimides (NDIs) with a heterocyclic 1,4-dihydro-2,3-pyrazinedione moiety have been synthesized from both 2,6-dibromonaphthalene and 2,3,6,7-tetrabromonaphthalene bisanhydrides by means of a stepwise protocol including imidization, nucleophilic displacement of the bromine atoms by ethane-1,2-diamine, in situ reductive dehalogenation, and further oxidation. These heterocycles (R = *n*-pentyl, cyclohexyl) are yellow dyes with green emission in organic solvent, where the acid form dominates. The orange nonfluorescent conjugate base can be generated quantitatively by CH₃COONBu₄ addition in DMSO, where it exhibits a p*K*_a = 7.63. The conjugate base becomes the only detectable species (by UV–vis spectroscopy), in water solution, even under acid conditions (pH 1). In aqueous DMSO the acid/base equilibrium is a function of the DMSO/water ratio. The unexpected acidity of these heterocyclic NDIs, which justifies the reactivity with CH₂N₂, has been rationalized by DFT computational means [PBE0/6-31 + G(d,p)] in aqueous solvent (PCM models) as a result of a strong specific solvation effect, modeled by the inclusion of three water molecules.

Introduction

1,4,5,8-Naphthalenetetracarboxylic acid diimides (NDIs) and their core-substituted derivatives have been a thoroughly investigated class of compounds in the last decades.¹ Such an interest is motivated by their numerous applications in material science due to their semiconducting properties.² Since NDIs can be reversibly reduced to stable radical

anions, under mild conditions,³ they have been exploited as electron-acceptor moieties in artificial light-harvesting systems.⁴ In supramolecular chemistry, several catenanes, rotaxanes, and self-assembling systems have been designed and synthesized around NDI cores.⁵

NDIs also attracted a great deal of interest in biological and medical areas as DNA intercalating agents.⁶ In addition,

(1) (a) Bhosale, S. V.; Jani, C. H.; Langford, S. J. *Chem. Soc. Rev.* **2008**, *37*, 331–342. (b) Grimshaw, J.; De Silva, A. P. *Chem. Soc. Rev.* **1981**, *10*, 181–203.

(2) (a) Kishore, R. S. K.; Kel, O.; Banerji, N.; Emery, D.; Bollot, G.; Mareda, J.; Gomez-Casado, A.; Jonkheijm, P.; Huskens, J.; Maroni, P.; Borkovec, M.; Vauthey, E.; Sakai, N.; Matile, S. *J. Am. Chem. Soc.* **2009**, *131*, 11106–11116. (b) Katz, H. E.; Lovinger, A. J.; Johnson, J.; Kloc, C.; Siegrist, T.; Li, W.; Lin, Y.-Y.; Dodabalapur, A. *Nature* **2000**, *404*, 478–481. (c) Würthner, F. *Angew. Chem.* **2001**, *113*, 1069–1071. (d) Takenada, S.; Uto, Y.; Saita, M.; Kondo, H.; David, W. *Chem. Comm.* **1998**, 1111–1112.

(3) (a) Di Antonio, M.; Doria, F.; Mella, M.; Merli, D.; Profumo, A.; Freccero, M. *J. Org. Chem.* **2007**, *72*, 8354–8360. (b) Heywang, G.; Born, L.; Fitzky, H.-G.; Hassel, T.; Hocker, J.; Müller, H.-K.; Pittel, B.; Roth, S. *Angew. Chem., Int. Ed.* **2004**, *43*, 668–698. (c) Zhong, C. J.; Kwan, W. S. V.; Miller, L. *Chem. Mater.* **1992**, *4*, 1423–1428.

(4) (a) El-Khouly, M. E.; Kim, J. H.; Kay, K.-Y. C.; Chan, S.; Ito, O.; Fukuzumi, S. *Chem.—Eur. J.* **2009**, *15*, 5301–5310. (b) Röger, C.; Yuliya, M.; Brunner, D.; Holzwarth, A. R.; Würthner, F. *J. Am. Chem. Soc.* **2008**, *130*, 5929–5939.

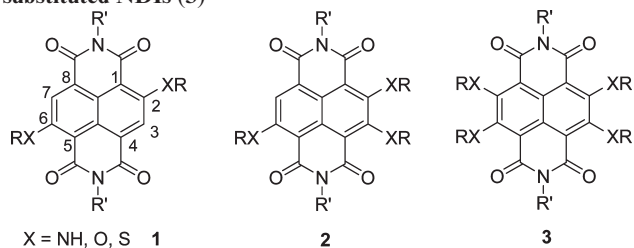
the propensity of NDIs to form excimers propelled the development of NDI-based fluorescent probes for sensitive and selective DNA detection.⁷

Very recently, tetrasubstituted naphthalene diimides, containing two polar or cationic substituents on the NDI core have been developed as a new class of promising ligands toward human telomeric quadruplex DNA (G-quadruplex). They showed selectivity over duplex DNA, inducing senescence in cancer cell lines typical of telomere-directed effects.⁸

Functionalization of NDIs by core substitution has been used by Würthner's group to induce a structural mediated tuning in the optical and redox properties of this class of dyes, extending the scope of their application.⁹

Synthetically di- and trisubstituted NDIs at the aromatic core are accessible from 2,6-dichloronaphthalene dianhydride by imidization with primary amines, followed by substitution of the chlorine atoms at the naphthalene core.¹⁰ A great variety of core 2,6-di- and 2,3,6-trisubstituted NDIs (see Chart 1 for numbering) have been synthesized starting from 2,6-dichloro- or 2,6-dibromonaphthalene dianhydride.^{10c,11,12} Very recently, NDIs bearing four electron-donating substituents at the naphthalene core (Chart 1) have been reported using 2,3,6,7-tetrabromonaphthalene dianhydride as a precursor.^{13,14}

CHART 1. Core 2,6-Di- (1), 2,3,6-Tri- (2), and 2,3,6,7-Tetra-substituted NDIs (3)



(5) For selected examples, see: (a) Fallon, G. D.; Lee, M. A.-P.; Langford, S. J.; Nichols, P. J. *Org. Lett.* **2004**, *6*, 655–658. (b) Wang, X.-Z.; Li, X.-Q.; Shao, X.-B.; Zhao, X.; Deng, P.; Jiang, X.-K.; Li, Z.-T.; Chen, Y.-Q. *Chem.—Eur. J.* **2003**, *9*, 2904–2913. (c) Li, X.-Q.; Feng, D.-J.; Jiang, X.-K.; Li, Z.-T. *Tetrahedron* **2004**, *60*, 8275–8284. (d) Gunter, M. J.; Farquhar, S. M. *Org. Biomol. Chem.* **2003**, *1*, 3450–3457. (e) Johnstone, K. D.; Yamaguchi, K.; Gunter, M. J. *Org. Biomol. Chem.* **2005**, *3*, 3008–3017. (f) Gunter, M. J. *Eur. J. Org. Chem.* **2004**, *8*, 1655–1673. (g) Vignon, S. A.; Jarrosson, T.; Lijima, T.; Tseng, H.-R.; Sanders, J. K. M.; Stoddart, J. F. *J. Am. Chem. Soc.* **2004**, *126*, 9884–9885. (h) Hansen, J. G.; Feeder, N.; Hamilton, D. G.; Gunter, M. J.; Becher, J.; Sanders, J. K. M. *Org. Lett.* **2000**, *2*, 449–452. (i) Kieran, A. L.; Pascu, S. I.; Jarrosson, T.; Gunter, M. J.; Sanders, J. K. M. *Chem. Commun.* **2005**, 1842–1844. (j) Pantos, G. D.; Pengo, P.; Sanders, J. K. M. *Angew. Chem., Int. Ed.* **2007**, *46*, 194–197.

(6) (a) Chu, Y.; Hoffman, D. W.; Iverson, B. L. *J. Am. Chem. Soc.* **2009**, *131*, 3499–3508. (b) Lee, J.; Guelev, V.; Sorey, S.; Hoffman, D. W.; Iverson, B. L. *J. Am. Chem. Soc.* **2004**, *126*, 14036–14042. (c) Guelev, V.; Sorey, S.; Hoffman, D. W.; Iverson, B. L. *J. Am. Chem. Soc.* **2002**, *124*, 2864–2865. (d) Sato, S.; Takenaka, S. *J. Organomet. Chem.* **2008**, *693*, 1177–1185. (e) Takenaka, S.; Uto, Y.; Saita, H.; Yokoyama, M.; Kondo, H.; Wilson, W. D. *Chem. Comm.* **1998**, 1111–1112.

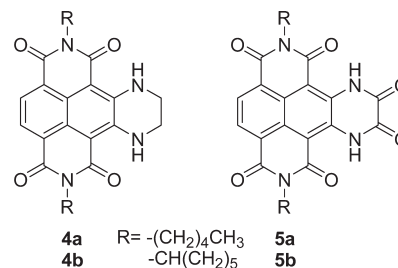
(7) (a) Lee, H. N.; Xu, Z.; Kim, S. K.; Swamy, K. M. K.; Kim, Y.; Kim, S.-J.; Yoon, J. *J. Am. Chem. Soc.* **2007**, *129*, 3828–3829. (b) Mokhir, A.; Krämer, R.; Wolf, H. *J. Am. Chem. Soc.* **2004**, *126*, 6208–6209.

(8) (a) Cuenca, F.; Greciano, O.; Gunaratnam, M.; Haider, S.; Munnur, D.; Nanjunda, R.; Wilson, W. D.; Neidle, S. *Bioorg. Med. Chem. Lett.* **2008**, *18*, 1668–1673. (b) Gunaratnam, M.; Swank, S.; Haider, S. M.; Galesa, K.; Reszka, A. P.; Beltran, M.; Cuenca, F.; Fletcher, J. A.; Neidle, S. *J. Med. Chem.* **2009**, *52*, 3774–3783.

(9) (a) Suraru, S.-L.; Würthner, F. *Synthesis* **2009**, 1841–1845. (b) Roger, C.; Miller, M. G.; Lysetska, M.; Miloslavina, Y.; Holzwarth, A. R.; Würthner, F. *J. Am. Chem. Soc.* **2006**, *128*, 6542–6543. (c) Banerji, N.; Furstenberg, A.; Bhosale, S.; Sisson, A. L.; Sakai, N.; Matile, S.; Vauthey, E. *J. Phys. Chem. B* **2008**, *112*, 8912–8922.

In an attempt to design new extended aromatics exhibiting a T-shaped planar structure, to be exploited as G-quadruplex ligands, we have combined an efficient two steps synthetic route to NDIs bearing cyclic substituents at the same side of the naphthalene core, at the 2,3 positions, yielding **4a** and **4b**, with an oxidative protocol generating tetraazabenzopyrene-1,3,6,8,10,11-hexaones (**5a** and **5b**, in Chart 2), bearing two different alkyl substituents at the imide moieties. The heterocycles **5a** and **5b** exhibit an unexpected acidity both in DMSO and in aqueous solution, which has been investigated experimentally and modeled by DFT computational means coupled with PCM solvation models.

CHART 2



Results and Discussion

Synthesis. Two different synthetic protocols have been used to achieve the syntheses of the heterocycle **4a**. The first one used 2,3,6,7-tetrabromonaphthalene dianhydride as starting material; the second one used the 2,6-dibromonaphthalene dianhydride. 2,3,6,7-Tetrabromonaphthalene dianhydride was prepared by bromination of naphthalene dianhydride with 2.5 equiv of dibromoisocyanuric acid (DBI) in oleum (20% SO₃) according to the procedure report by Würthner.¹⁴ The imidization of the anhydride by pentylamine and cyclohexylamine outlined in Scheme 1 was carried out in acetic acid. The tetrabromonaphthalene diimide **8a** was synthesized as a major product in low yield 40%, along with byproducts arising from complete or partial reductive dehalogenation **6a** (35%) and **7a** (26%). In order to improve the reaction yield of the diimide **8a**, another preparation was run in a dedicated microwave reactor, under atmospheric pressure, in an open reaction vessel. The reaction was carried out at 150 °C for a period of 30 min. Under these conditions, 100 W was the power required for 45 s to warm the reaction mixture at the desired temperature, followed by pulses of 45–50 W to maintain the reaction mixture at 150 °C. The microwave-assisted synthesis generates the imide adducts **8a**, in a much better yield (65%), reducing the dehalogenation byproducts.

The bromo NDIs **6a–8a** were then isolated by column chromatography and used as precursors for the next step of

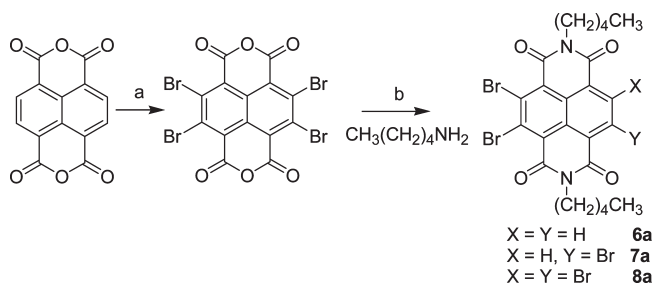
(10) (a) Thalacker, C.; Roger, C.; Würthner, F. *J. Org. Chem.* **2006**, *71*, 8098–8105. (b) Würthner, F.; Ahmed, S.; Thalacker, C.; Debaerdemaeker, T. *Chem.—Eur. J.* **2002**, *8*, 4742–4750.

(11) Jones, B. A.; Facchetti, A.; Marks, T. J.; Wasielewski, M. R. *Chem. Mater.* **2007**, *19*, 2703–2705.

(12) Chaignon, F.; Falkenstrom, M.; Karlsson, S.; Blart, E.; Odobel, F.; Hammarstrom, L. *Chem. Commun.* **2007**, 64–66.

(13) (a) Vollmann, H.; Becker, H.; Corell, M.; Streeck, H. *Liebigs Ann.* **1937**, *531*, 1–159. (b) Kishore, R. S. K.; Ravikumar, V.; Bernardinelli, G.; Sakai, N.; Matile, S. *J. Org. Chem.* **2008**, *73*, 738–740.

(14) Roger, C.; Würthner, F. *J. Org. Chem.* **2007**, *72*, 8070–8075.

SCHEME 1. Imidization of the 2,3,6,7-Tetrabromonaphthalene Bisanhydride by Pentylamine^a


^aReagents and conditions: (a) dibromoisocyanuric acid (DBI), oleum (20% SO_3), 25 °C, 3 h, yield 93%; (b) pentylamine 150 °C, 30 min, microwave assisted (**8a**, 65%, yield).

synthesis: a nucleophilic substitution of the halogen atoms with ethane-1,2-diamine (EDA).¹⁴ The nucleophilic aromatic substitution ($\text{S}_{\text{N}}\text{Ar}$) on both **6a** and **7a** gave **4a** in good yields ($\geq 85\%$), in DMF at 130 °C. The $\text{S}_{\text{N}}\text{Ar}$ reaction on **8a** was carried out using three different conditions: (a) in DMF, (b) in neat EDA, both at 130 °C with an oil bath, for 30 min, and (c) in DMF microwave-assisted (MW) at 150 °C, 250 psi, 200 W, 10 min, as outlined in Table 1. The ring-closure by two sequential $\text{S}_{\text{N}}\text{Ar}$, and the further reductive dehalogenation yielding **4a**, occurred in one pot in DMF in the presence of EDA at 130 °C for 30 min (Scheme 2). The product **11a** resulting from a complete $\text{S}_{\text{N}}\text{Ar}$, which is always a byproduct, was generated in higher yield in the microwave-assisted protocol. To improve the synthesis of **4a** minimizing the side-reaction products, we followed a more efficient synthetic route starting from 2,6-dibromonaphthalene dianhydride as depicted in Scheme 3. Since this second synthetic protocol is much more efficient than the first one, particularly for bulky R substituents, we used it also to synthesize **4b** and **5b**.

TABLE 1. Reactants and Conditions for the Nucleophilic Aromatic Substitution on Polybrominated NDIs 6a–8a and 12a

reactant	conditions ^a	products (% , yield)
6a	a DMF, Ar, 130 °C, 30 min	4a (92)
7a	a DMF, Ar, 130 °C, 30 min	4a (85), 10a (< 5%)
8a	b neat EDA, Ar, 130 °C, 30 min	9a (24), 4a (27), 11a (25)
8a	a DMF, Ar, 130 °C, 30 min	9a (3), 4a (86)
8a	c DMF, MW, 150 °C, 250 psi, 200 W, 10 min	9a (35), 4a (16), 11a (7)
8a	d neat EDA, Ar, rt, 16 h	4a (5), 10a (72)
12a	d neat EDA, Ar, rt, 16 h	4a (52), 10a (40)
12a	d neat EDA, Ar, rt, 2 h	4a (21), 14a (50), 10a (8)

^aIn neat ethane-1,2-diamine (EDA) or in DMF.

The 2,6-dibromo-substituted NDIs **12a** and **12b** were synthesized by a classical method of imidation of the 2,6-dibromo-1,4,5,8-naphthalenetetracarboxylic acid dianhydride. The following $\text{S}_{\text{N}}\text{Ar}$ yielding **14a** and subsequent ring-closure was carried out in neat EDA, at room temperature (condition d, in Table 1), following a similar procedure used by Würthner for the functionalization of 2,6-dichloro NDIs.¹⁵ The reaction was monitored by reversed-phase HPLC. The reactant **12a** was converted into the monosubstituted adduct **14a** after 2 h. The following

(15) Roger, C.; Ahmed, S.; Würthner, F. *Synthesis* **2007**, 12, 1872–1876.

ring closing (step iii, in Scheme 3), leading to a mixture of products **4a** and **10a** was quantitative after an additional 14 h at rt. The cyclization reaction could be an intramolecular conjugate addition of the NH_2 group to the ortho position, with the aromatic ring bearing the amide moiety acting as Michael acceptor, followed by an oxidative aromatization.¹⁶ Since more than 50% of the adduct arising from the cyclization in the mixture is dehalogenated, the NDI core acts as the main oxidizing agent. The final step (iv, in Scheme 3) was a mild and quantitative reductive dehalogenation, of both the monobromo derivatives **10a** and **10b**, in aqueous DMSO by $\text{Na}_2\text{S}_2\text{O}_4$ to afford **4a** and **4b**, which were used, without purification, to prepare the diamide analogues **5a** and **5b**.

Scheme 4 shows the final oxidative step of the synthesis. To our knowledge, this oxidation is a novelty in the current literature. The closest reaction reported in the literature is the oxidation of the 1*H*-quinoxalin-2-one to 1,4-dihydroquinoxaline-2,3-dione by permanganate.¹⁷ Several oxidants have been used such as DDQ, Dess–Martin, and Jones, of which only the latter successfully oxidized the reagents into the dicarbonyl products **5a** and **5b** in fairly good yields (75%).

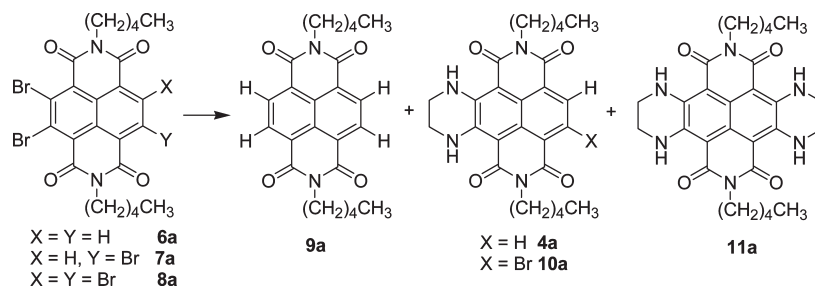
Reactivity of 5a toward CH_2N_2 . It has been previously shown that heterocycles such as 2,3-dihydroxyquinoxalines and 2-pyridones can slowly react with diazomethane to afford in low yield both *O*- and *N*-methylation, only in the presence of acid silica gel catalysis.¹⁸ In contrast, the heterocycle **5a** reacts instantaneously with diazomethane in organic solvents (Et_2O and CH_2Cl_2), with N_2 generation, exhibiting a behavior very similar to that of a carboxylic acid. By controlling the reaction time it has been possible to selectively generate the monomethylated and the bis-methylated adducts **15a** and **16a** (Scheme 5). The *O*-methylated adducts have been used as standards to investigate the tautomeric and acid–base equilibriums of **5a** and **5b** in organic solvents and in aqueous media by UV–vis spectroscopy.

Spectroscopic Properties in Organic and Aqueous Solvents. Absorbance and Emission Spectra. In order evaluate the possibility of exploiting the new NDIs as a fluorescent chemosensor, and more specifically as probes for G-quadruplex sensing, we decided to measure the absorbance and emission spectra of the NDIs **5a** and **5b** and their precursors **4a** and **4b**. The disubstituted NDI **4a** is a green fluorescence compound (Figure 1a, $\lambda_{\text{max}} = 498 \text{ nm}$) with an absorption spectra characterized by an electronic transition in the 400–550 nm range, with $\lambda_{\text{max}} = 488 \text{ nm}$ (Figure 1a). Compared to 2,6-dialkylamino NDIs synthesized by Würthner ($\lambda_{\text{max}} = 620 \text{ nm}$),^{10a} the absorption maximum is blue-shifted by 132 nm. The UV–vis property of **4a** is much more similar to that of 2,6-dialkoxy NDIs ($\lambda_{\text{max}} = 470 \text{ nm}$).^{10a} This evidence suggests that cyclic amine substituents at 2,3 positions on the NDI core are less efficient electron donor than the conformational flexible acyclic amine moieties at 2,6 positions. After the oxidation, the UV–vis spectra of the resulting **5a** (Figure 1b) is 34 nm blue-shifted in comparison to the spectra of **4a** (Figure 1a). Compound **5a** exhibits an

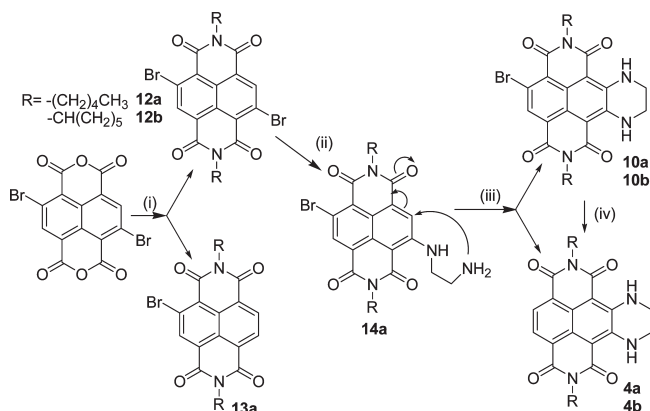
(16) An intermediate resulting from the cyclization step (iii) in Scheme 3 was detected by ^1H NMR in CDCl_3 . The structural characterization and its decay are currently under investigation.

(17) Obafemi, C. A.; Pfeleiderer, W. *Helv. Chim. Acta* **1994**, 77, 1549–56.

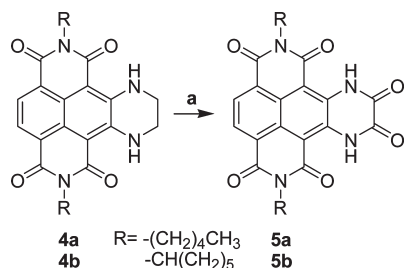
(18) (a) Nishiyama, H.; Nagase, H.; Ohno, K. *Tetrahedron Lett.* **1979**, 48, 4671–4674. (b) Cheeseman, G. W. H. *J. Chem. Soc.* **1955**, 1804–1809.

SCHEME 2. Nucleophilic Aromatic Substitution on Polybromo-NDIs^a

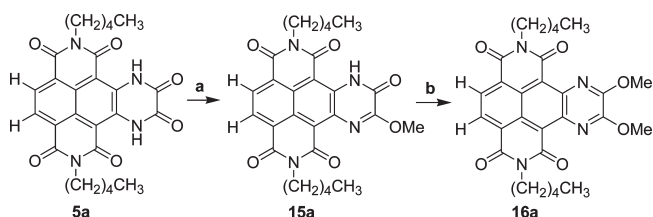
^aReagents and conditions are shown in Table 1.

SCHEME 3. Synthesis of 4a and 4b according to the Second Synthetic Protocol^a

^aReagents and Conditions: (i) pentylamine, CH_3COOH , 130°C , 30 min; (ii) EDA, 25°C , 2 h, Ar; (iii) EDA, 25°C , 14 h, Ar; (iv) $\text{Na}_2\text{S}_2\text{O}_4$, DMSO/ $\text{H}_2\text{O} = 20:80$, 40°C , 2 h, Ar.

SCHEME 4. Oxidation of 4 to 5^a

^aConditions: (a) $\text{K}_2\text{Cr}_2\text{O}_7$, H_2SO_4 , $\text{H}_2\text{O}/\text{acetone}$, 100°C , 2 h.

SCHEME 5^a

^aReagent and conditions: (a) CH_2N_2 , CHCl_3 , rt, 30 s; (b) CH_2N_2 , CHCl_3 , rt, 10 min.

intense cyan (blue-green) bright fluorescence emission (Figure 1b), more intense than **4a**. The absorption and

emission spectra of the NDI **5b** are almost superimposable on that of **5a** (Supporting Information).

The UV–vis spectra of both NDI **5a** and **5b** were investigated in several organic solvents: benzene, CHCl_3 , methanol, acetonitrile (ACN) (Figure 2a), DMSO, and aqueous DMSO (Figure 2b).

The absorbance spectra in organic solvents is not substantially affected by the polar or protic nature of the solvent, since in the above solvents including DMSO the spectra are very similar (for **5a** see Figures 2a and 2b, red line). The appearance of a new absorbance in water (Figure 2b, blue line) reveals the presence of another additional chemical species, which is in equilibrium with **5a**, as suggested by the two isobestic points at 366 and 469 nm in the spectra recorded in aqueous DMSO (Figure 2c). The equilibrium is shifted progressively toward the new species increasing the water ratio, which becomes the most populated in water containing a small amount of DMSO (2%) (Figure 2b). The comparison of the UV–vis spectra of the new species in water to the spectra of both the mono- and the dimethoxy-substituted heterocycles **15a** and **16a** (Figure 3a), suggests that the new species is not a tautomer of the diamide **5a**. On the other hand, the addition of a weak base, such as triethylamine (TEA, 0.3 equivalents), to a solution of **5a** in CHCl_3 changes the spectra generating a new band with two absorption maxima ($\lambda_{\text{max}} = 487, 509$ nm, Figure 3b), which are fairly similar to those of the new species in water solution ($\lambda_{\text{max}} = 485, 495$ nm). The effect of triethylamine (TEA, 1 equiv) or $\text{CH}_3\text{COONBu}_4$ on the spectra, generating a new red-shifted absorption with two maxima in DMSO ($\lambda_{\text{max}} = 521, 549$ nm), and in ACN ($\lambda_{\text{max}} = 521, 549$ nm), suggests that the heterocycles **5a** in organic solvents is quantitatively deprotonated by a weak base, and the new bands have to be assigned to the anion **5aA** (Scheme 6) free or as ion pair with the triethylammonium cation.

It is worth noting that the efficient solvation of the triethylammonium cation leaves the anion **5aA** free in DMSO, resulting in a UV–vis spectrum red-shifted by 70 nm in comparison to the spectrum in chloroform where the ion pair **5aA**/triethylammonium cation is present. Efficient ion-pair separation results in a progressive red shift of the UV–vis absorbance of the anion **5aA** (passing from chloroform, ACN, and DMSO in the presence of TEA). Due to the similarity of the spectra in water to that in chloroform in the presence of TEA, we suggest that the new absorbance in water solution has to be ascribed to the anion **5aA**.

The NDI **5b**, with the more bulky cyclohexyl substituents replacing the *n*-pentyl groups at the imide nitrogen atoms, mirrors the behavior of **5a**, with the generation of an anion

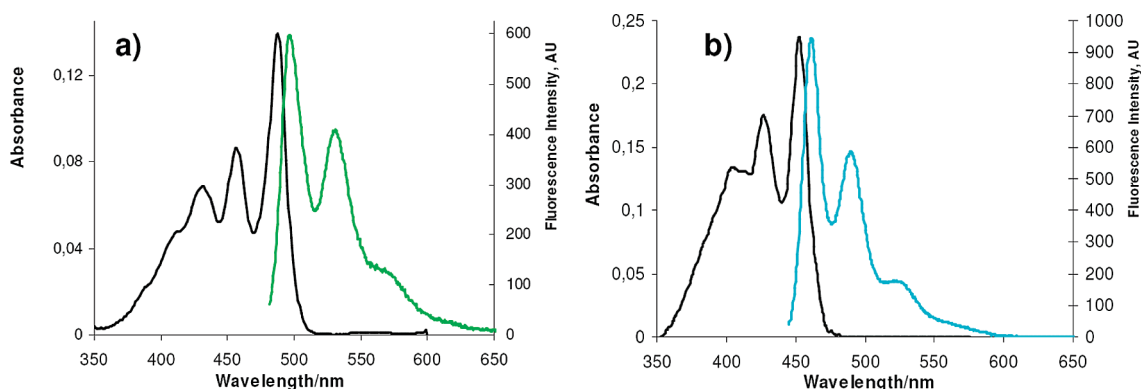


FIGURE 1. (a) UV-vis absorption (black lines) and fluorescence spectra (colored lines) of (a) **4a** (10^{-5} M) and (b) **5a** (2×10^{-5} M).

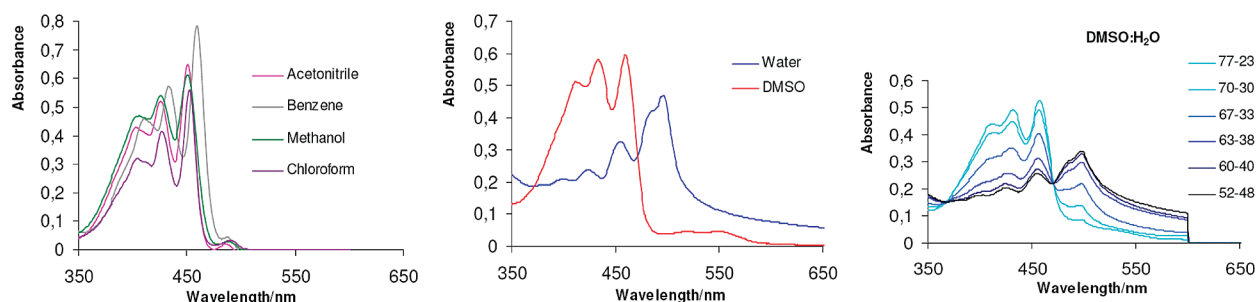


FIGURE 2. (a) UV-vis absorption spectra of **5a** in ACN (6×10^{-5} M), benzene, CH₃OH and CHCl₃. (b) UV-vis absorption spectra of **5a** in DMSO (5×10^{-5} M, red line) and in water/DMSO = 98:2 (blue line). (c) UV-vis absorption spectra of **5a** in aqueous DMSO (5×10^{-5} M) from 77:23 to 52:48 DMSO/water volume ratio.

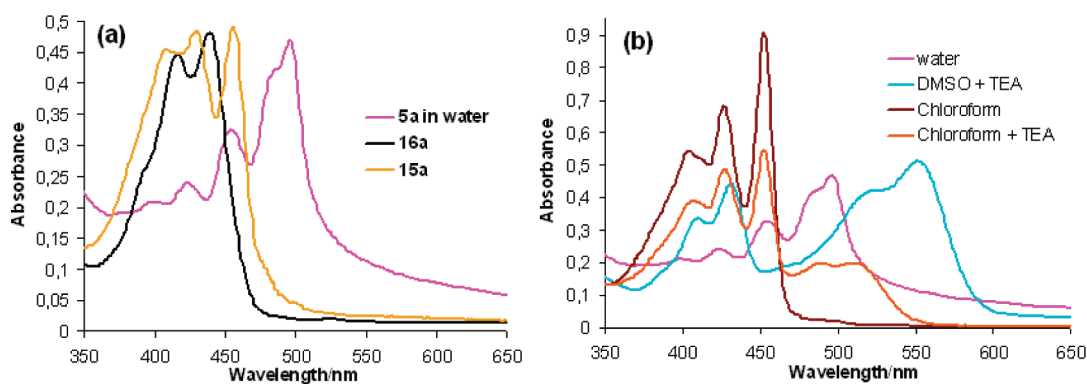
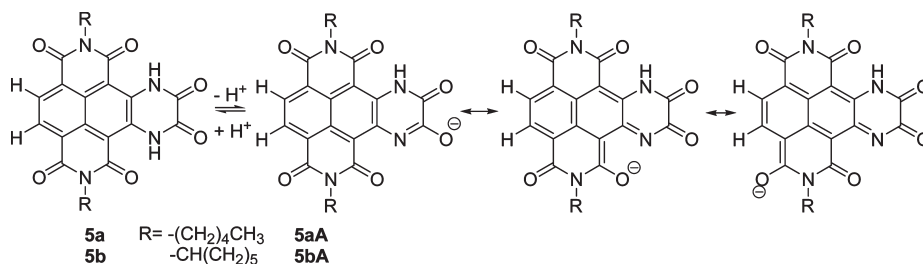


FIGURE 3. (a) UV-vis spectra of **5a** in water (3×10^{-5} M), **15a** and **16a** in chloroform (3×10^{-5} M). (b) UV-vis spectra of **5a** in water (3×10^{-5} M, fuchsia), in neat chloroform (5×10^{-5} M, brown), in chloroform with TEA (0.3 equiv, orange), and in DMSO with TEA (1 equiv, cyan).

SCHEME 6. Acid-Base Equilibrium Involving **5a,b** and Their Conjugate Bases **5aA** and **5bA**



5bA in water solution. For a comparison of the UV-vis absorbance of the two anions **5aA** and **5bA**, see Figure 4. Although the more bulky cyclohexyl substituent slightly

reduces the tailing of the UV-vis spectra over 500 nm (probably caused by clustering of the conjugate base with the acid), the shape and the maxima of the two spectra are

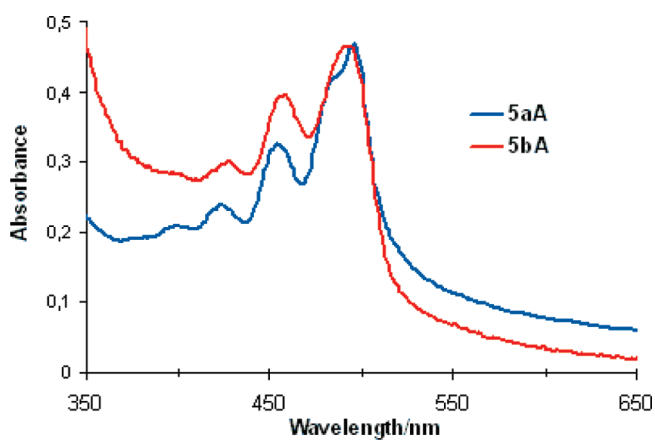


FIGURE 4. UV-vis spectra of the anions **5aA** (3×10^{-5} M) (blue line) and **5bA** (red line) in water solution.

very similar. The maxima in the UV-vis spectra are unaffected by concentration in the 10^{-4} – 10^{-5} M range.

NDI Acidity Measurements. The UV-vis spectra of **5a** change for the addition of an equimolar amount of TEA in DMSO as a consequence of the equilibrium depicted in Scheme 6. The titration of **5a**, using $\text{CH}_3\text{COONBu}_4$ as a base in DMSO (Figure 5), gave a $\text{p}K_a$ 7.63, which is 10 orders of magnitude lower than the $\text{p}K_a$ of 2-pyridone in DMSO ($\text{p}K_a$ 17.0).¹⁹

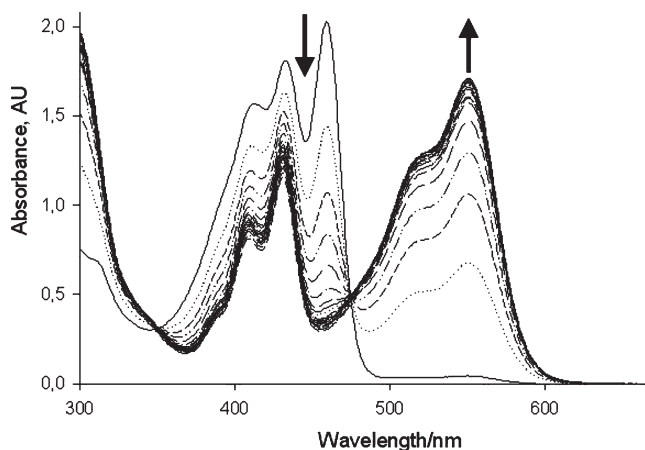


FIGURE 5. Absorption spectra of a DMSO solution of **5a** (1×10^{-4} M) measured during a titration with $\text{CH}_3\text{COONBu}_4$.

The UV-vis absorbance of **5aA** does not change in water solution in the pH range 1–8. Therefore, it has not been possible to measure the $\text{p}K_a$ of **5a** in water solution since it should be lower than 1.

Computational Acidity. In order to evaluate the acidity of the NDIs **5a** and to describe the effect of water as solvent on the acidity, we have computed the $\text{p}K_a$ of a prototype NDI model (**NDIH**, exhibiting methyl substituents, on both the imide moieties, see Scheme 7) by a semiempirical computational strategy, which has been used successfully to evaluate the $\text{p}K_a$ for twisted amide²⁰ and unstable cyclopropylpyrroleindoles.²¹ Considerable cancellation of errors is expected if relative $\text{p}K_a$

are evaluated instead of absolute $\text{p}K_a$. This requires the choice of a similar reference molecule, in our case, 1,4-dihydro-2,3-quinoxalinedione (**QXH**). **QXH** is a cyclic bis-amide (Scheme 7) exhibiting structural and electronic features quite similar to those of the model NDI, for which the experimental $\text{p}K_a$ has been experimentally measured. The experimental $\text{p}K_a$ value measured in water [$\text{p}K_a(\text{exp})(\text{QXH})$] is 9.27, in good agreement with previously published data (9.52, 9.75).²² The $\text{p}K_a$ of the model **NDIH** has been calculated from the computed ΔG_{aq} value for the proton-transfer reactions in Scheme 7 and the experimental $\text{p}K_a$ of **QXH**, according to eq I.

$$\text{p}K_a(\text{NDIH}) = \Delta G_{\text{aq}}/RT \ln 10 + \text{p}K_a(\text{exp})(\text{QXH}) \quad (\text{I})$$

Two different proton-transfer reaction models (a) and (b) have been considered (Scheme 7). The most simple one (a) does not include any water molecules. The second proton-transfer reaction model (b) includes three water molecules H-bonded to each acid/base couple. The choice of the “three water molecules model” is the compromise between the needs to contain the molecular complexity of the water cluster and to describe the specific solvation involving the most negatively charged atoms of the anion **NDI**[−]. The second model has been suggested by the fact that error of the PCM method in the predictions of acidities in water may become as large as 7 $\text{p}K_a$ units, if the solvent–solute interactions (mainly due to hydrogen bonding) in the first solvation shell are neglected.²³ A remedy for this problem was to use a cluster-continuum model.²⁴ This cluster-continuum model is a hybrid approach that combines gas-phase clustering by explicit solvent molecules and solvation of the cluster by the dielectric continuum. Using the cluster-continuum model, $\text{p}K_a$ between −10 and 50 for 17 acids in aqueous solution were calculated with an error of 2.2 $\text{p}K_a$ units.²³ The above results have clearly demonstrated that, by using the PCM method, one is able to predict the $\text{p}K_a$ in aqueous solution with a precision of about 0.5–2.2 $\text{p}K_a$ units. Therefore, the cluster-continuum model should allow a better evaluation of the solvation effects of water on the NDI acidity. Bulk solvation effects have been computed for both models (a) and (b) optimizing the acid and conjugate base structures in the solvent bulk by PCM solvation model at PBE0/6-31+G(d,p) level of theory,²⁵ using UAHF-rad.ii.²⁶

Geometries in Gas Phase and in Water Bulk. In the model (a), all the structures, with the exception of the anion **NDI**[−], are planar. The nonplanarity of the anion **NDI**[−] is due to the strong electrostatic repulsion between the nitrogen and oxygen atoms, both negatively charged. The effect of the solvent bulk reduces significantly the out of plane bending of the carbonyl moiety relative to the dihydropyrazine ring. Model (b) appeared to be computationally more demanding since the three water molecules are loosely bound to the heterocycles by a H-bonding network with great

(22) Albert, A.; Phillips, J. N. *J. Chem. Soc.* **1956**, 1294–1304.

(23) Pliego, J. R., Jr.; Riveros, J. M. *J. Phys. Chem. A* **2002**, *106*, 7434–7439.

(24) Pliego, J. R., Jr.; Riveros, J. M. *J. Phys. Chem. A* **2001**, *105*, 7241–7247.

(25) (a) Saracino, G. A. A.; Improta, R.; Barone, V. *Chem. Phys. Lett.* **2003**, *411*–415. (b) Adamo, C.; Barone, V. *J. Chem. Phys.* **1999**, *110*, 6158–6170. (c) Cimino, P.; Gomez-Paloma, L.; Barone, V. *J. Org. Chem.* **2004**, *69*, 7414–7422.

(26) Barone, V.; Cossi, M.; Tomasi, J. *J. Chem. Phys.* **1997**, *108*, 3210–3221.

(19) Bordwell, F. G. *Acc. Chem. Res.* **1988**, *21*, 456–463.

(20) Mujika, J. I.; Mercero, J. M.; Lopez, X. *J. Phys. Chem. A* **2003**, *107*, 6099–6107.

(21) Freccero, M.; Gandolfi, R. *J. Org. Chem.* **2005**, *70*, 7098–7106.

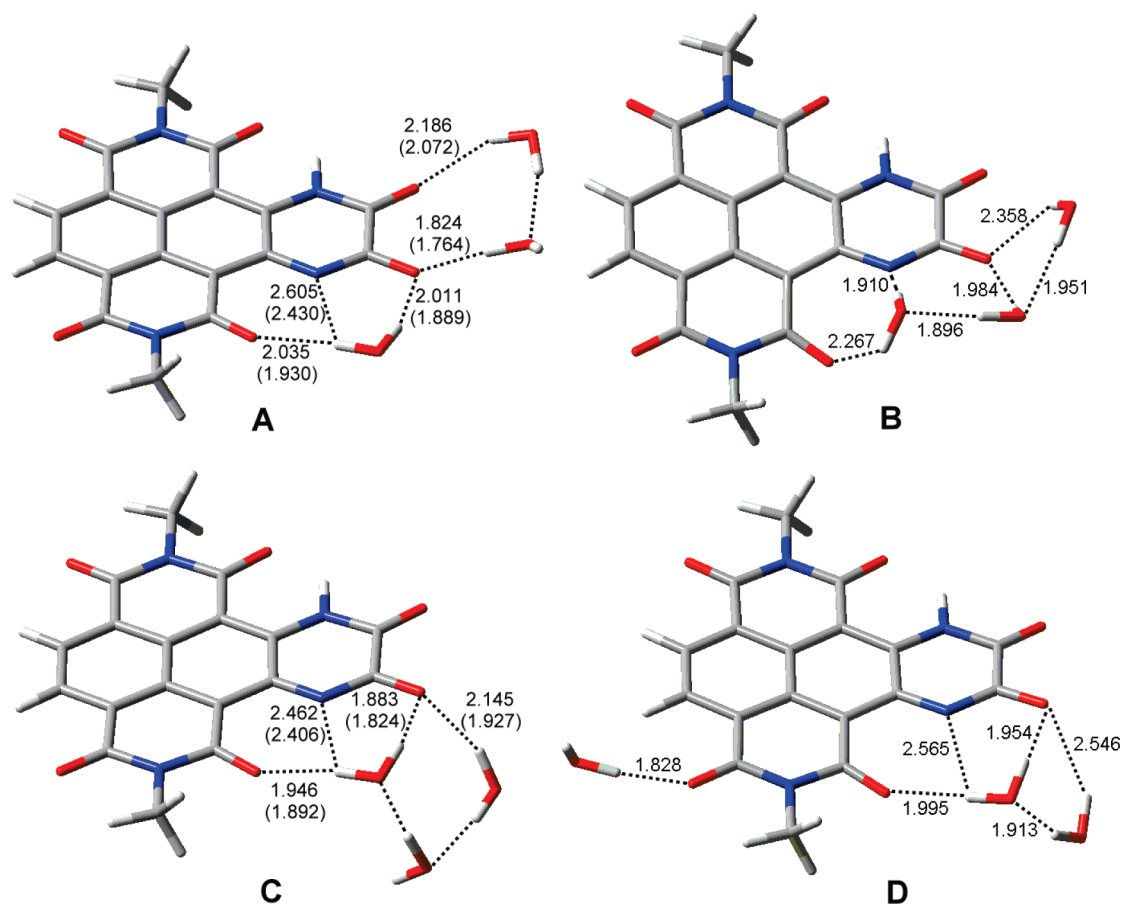
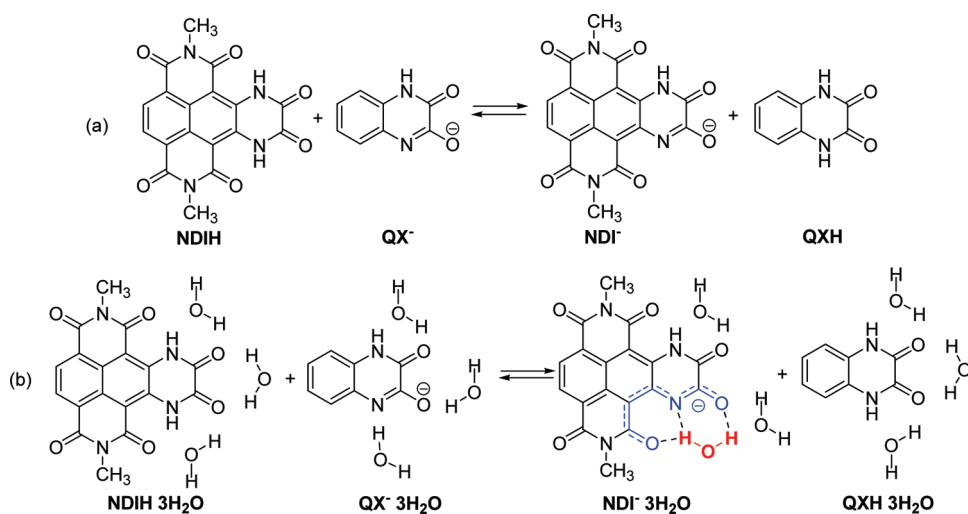


FIGURE 6. Geometries in the gas phase and in water bulk (in parentheses, PCM model, UAHF radii) for the model anion $\text{NDI}^- \cdot 3\text{H}_2\text{O}$ in the presence of three water molecules at the PBE0/6-31+G(d,p) level of theory.

SCHEME 7. Proton-Transfer Reaction without (a) and with Three Water Molecules H-Bonded to Each Acid/Base Couple (b) Used as Models for the Computational Evaluation of the $\text{p}K_a$ of 5a



conformational mobility. Actually, we were able to locate only one conformational minima both in the gas phase and in solvent bulk for the three stationary points $\text{QXH} \cdot 3\text{H}_2\text{O}$, $\text{QX}^- \cdot 3\text{H}_2\text{O}$, and $\text{NDIH} \cdot 3\text{H}_2\text{O}$ (Scheme 7). On the other hand we were able to locate four relative minima for the conjugate base $\text{NDI}^- \cdot 3\text{H}_2\text{O}$ in gas phase (A–D in Figure 6), all exhibiting a

planar structure. Optimization in water bulk was successful only for the two most stable water complex A and C. In the two most stable $\text{NDI}^- \cdot 3\text{H}_2\text{O}$ complexes, including three water molecules, the “anionic cavity” in the heterocyclic structure (in blue, Scheme 7) tightly binds a coplanar water molecule, with three H-bonding interactions (Figure 6).

TABLE 2. Electronic Energies (Hartree), in the Gas Phase (E_{gas}), Thermal Correction to Gibbs Free Energy in the Gas Phase (δG_{gas}), Gibbs Free Energy in the Gas Phase (G_{gas}), and Aqueous Solution (G_{aq}) at the PBE0/6-31+G(d,p) Level of Theory with PCM Solvation Models

compd	E_{gas}	δG_{gas}	G_{gas}	G_{aq}
QX ⁻	-567.300039	0.086272	-567.213767	-567.398792
QXH	-567.8494478	0.100720	-567.748728	-567.875130
NDI ⁻	-1360.4827393	0.205033	-1360.277706	-1360.558389
NDIH	-1361.0147537	0.220398	-1360.794356	-1361.019470
including specific interactions with 3 H₂O				
QX ⁻ 3H ₂ O	-796.4192348	0.148900	-796.270335	-796.496536
QXH 3H ₂ O	-796.9458311	0.162589	-796.783242	-796.968522
NDIH 3H ₂ O	-1590.092377	0.278762	-1589.813615	-1590.115295
NDI ⁻ 3H ₂ O	-1589.5912688 ^a	0.266906	-1589.324363 ^a	-1589.660287 ^a
	-1589.5911693 ^b			
	-1589.5950532 ^c	0.270646	-1589.324407 ^c	-1589.663297 ^c
	-1589.5872889 ^d			

^aConformer A. ^bConformer B. ^cConformer C. ^dConformer D, in Figure 6.

From a geometrical point of view, the H-bonding network becomes more tight passing from gas phase to water bulk, with the H-bonding between water and the anion NDI⁻ shorter in condensed phase than in gas phase. This aspect suggests that the specific interactions between the water molecules and the anions **5aA** and **5bA** are stronger than in QX⁻ 3H₂O, due to an “anionic cavity”, which for its size and charge binds a water molecule.

Energy in Gas Phase and in Water Bulk. The energy data in Table 2 have been used to calculate the free energy for the proton exchange reactions (a) and (b) depicted in the Scheme 7, both in the gas phase and in the solvent bulk (Table 3). These data suggest that the reactions (a) and (b) are very exoergic by more than 10 kcal/mol. Using the eq 1 and the experimental pK_a value (9.27) measured for the reference acid/base couple QXH/QX⁻, in water, we have been able to estimate the pK_a of **5a** in water solution. The model (a) which takes into account only the bulk effect of the solvent suggests a pK_a 1.8. The more refined model (b), which uses proton exchange between water clusters, including specific interactions, suggests a lower value (pK_a 0.1, Table 3). These data unequivocally explain why the anions **5aA** and **5bA** are still the main species in water solution at pH ≥ 1.

TABLE 3. Free Energy for the Proton Exchange Reaction in Scheme 7 in the Gas Phase and in Aqueous Solution with and without Three Water Molecules [at PBE0/6-31+G(d,p) Level of Theory with PCM Solvation Models]^a

	gas phase	gas phase + 3H ₂ O	water bulk	water bulk + 3H ₂ O
ΔG	-11.5	-14.8	-10.2	-12.5
pK _a		-1.6	1.8	0.1

^aThe pK_a of the prototype NDIH was computed according to eq 1.

Conclusion

In summary, this investigation describes the synthesis of new heterocyclic dihydropyrazinediones starting from both 2,6-dibromonaphthalene and 2,3,6,7-tetrabromonaphthalene bisanhydride by a stepwise protocol including imidization, aromatic nucleophilic substitution by ethane-1,2-diamine, in situ reductive dehalogenation, and oxidation. These new heterocycles exhibit a strong green fluorescence in organic solvents including DMSO, revealing an unexpected acidity both in DMSO (pK_a 7.6) and in water (pK_a < 1). A computational investigation at PBE0/6-31+G(d,p) level of theory, using PCM solvation models, predicts for a model NDI a pK_a value close to zero, as a result of both

the electron-withdrawing nature of the NDI core and the strong specific solvation by water. Therefore, both the new NDIs **5a** and **5b** exist mainly as non fluorescent conjugate bases in water solution at pH ≥ 1, which exhibit an “anionic cavity” on the heterocyclic structures. Along this line, we are currently exploring other NDI analogues exhibiting two cationic arms to be developed as new G-quadruplex ligands.

Experimental Section

2,3,6,7-Tetrabromo- and 2,6-dibromonaphthalene dianhydride were synthesized via standard published procedures.^{14,10c}

Procedure for the Synthesis of 6a, 7a, and 8a. To a stirred suspension of 2,3,6,7-tetrabromodianhydride (600 mg, 0.001 mol) in glacial acetic acid (15 mL) was added pentylamine (1.6 mL). After being stirred for 30 min at 130 °C, the reaction mixture was cooled to room temperature and put into ice to induce precipitation. The crude orange solid was filtered on a Hirsch filter and purified by column chromatography (CH₂Cl₂), yielding **6a** (35%), **7a** (26%), and **8a** (21%).

Microwave-Assisted Synthesis of 7a and 8a. The reaction was run in a dedicated microwave reactor (CEM Discover model, with PC control) under atmospheric pressure in an open reaction vessel. The microwave method was power-controlled (100 W, power input) to maintain the desired temperature (150 °C). An IR noncontact sensor was used for temperature measurement of vessel contents. To a stirred suspension of 2,3,6,7-tetrabromodianhydride (600 mg, 0.001 mol) in glacial acetic acid (25 mL) was added pentylamine (1.6 mL). After being stirred for 30 min, the reaction mixture was cooled to room temperature and quenched in ice to induce a precipitation. The crude yellow solid was filtered on a Hirsch filter and purified by column chromatography (CH₂Cl₂), yielding **7a** (14%) and **8a** (65%).

N,N'-Dipentyl-2,3-dibromonaphthalene-1,4,5,8-tetracarboxylic Acid Bisimide (6a). Orange solid. ¹H NMR (300 MHz, CDCl₃, 25 °C, TMS): δ 8.98 (s, 2H), 4.20 (t, J = 7.4 Hz, 4H), 1.73 (broad s, 4H), 1.41 (broad s, 8H), 0.92 (t, J = 6.0 Hz, 6H). ¹³C NMR (300 MHz, CDCl₃, 25 °C, TMS): δ 160.61; 138.94; 128.21; 127.61; 125.24; 123.98; 41.46; 29.05; 27.46; 22.25; 13.85. MS (EI): m/z calcd for C₂₄H₂₄Br₂N₂O₄ 562.01, found 564.27. Anal. Calcd: C, 51.09; H, 4.29; Br, 28.32; N, 4.96; O, 11.34. Found: C, 51.20; H, 4.22; Br, 28.15; N, 5.00.

N,N'-Dipentyl-2,3,6-tribromonaphthalene-1,4,5,8-tetracarboxylic Acid Bisimide (7a). Pink solid. ¹H NMR (300 MHz, CDCl₃, 25 °C, TMS): δ 9.01 (s, 1H), 4.20 (t, J = 7.4 Hz, 4H), 1.73 (broad s, 4H), 1.41 (broad s, 8H), 0.92 (t, J = 6.0 Hz, 6H). ¹³C NMR (300 MHz, CDCl₃, 25 °C, TMS): δ 160.64; 151.73; 138.94; 138.19; 128.22; 127.61; 125.23; 123.96; 120.43; 41.48; 29.06; 27.46; 22.27; 13.87. MS (EI): m/z calcd for C₂₄H₂₃Br₃N₂O₄ 643.16, found

644.27. Anal. Calcd: C, 44.82; H, 3.60; Br, 37.27; N, 4.36; O, 9.95. Found: C, 44.80; H, 3.65; Br, 37.32; N, 4.41.

***N,N'*-Dipentyl-2,3,6,7-tetrabromonaphthalene-1,4,5,8-tetracarboxylic Acid Bisimide (8a)**. Yellow solid. ^1H NMR (300 MHz, DMSO- d_6): δ 4.13 (m, 4H), 1.73 (broad s, 4H), 1.41 (broad s, 8H), 0.92 (t, J = 6.0 Hz, 6H). MS (EI): m/z calcd for $\text{C}_{24}\text{H}_{22}\text{Br}_4\text{N}_2\text{O}_4$ 722.06, found 723.05. Anal. Calcd: C, 39.92; H, 3.07; Br, 44.26; N, 3.88; O, 8.86. Found: C, 40.00; H, 3.15; Br, 44.28; N, 3.91.

Thermal Procedure for a Ring-Closure Nucleophilic Substitution. Reaction Conditions (a). The reactant **8a** (150 mg, 0.0002 mol) was heated under argon in DMF with ethane-1,2-diamine (48 mg, 0.0008 mol) at 135 °C for 30 min. After this period, the solution became brownish and then was quenched in ice to induce precipitation of the product. The crude was purified by column chromatography (Cy/AcOEt = 8:2) to yield **9a** (3%) and **4a** (86%).

Reaction Conditions (b). The reactant **8a** (150 mg, 0.0002 mol) was heated under argon in ethane-1,2-diamine (15 mL) at 135 °C for 30 min. After this period, the solution became brownish and then was cooled to room temperature, water was added (50 mL), and the solution was extracted with CH_2Cl_2 (3 \times 50 mL). The combined organic phases were washed with 1 N HCl. The solvent was then removed under vacuum and purified by column chromatography ($\text{CHCl}_3/\text{MeOH}$ 9:1), yielding **9a** (24%), **4a** (27%), and **11a** (25%).

Reaction Conditions (c), Microwave-Assisted in a Closed Vessel. Compound **8a** (150 mg, 0.0002 mol) was heated in a closed vessel in DMF with ethane-1,2-diamine (48 mg, 0.0008 mol) at 170 °C for 10 min, 200 psi, with a power of 200 W. After this period, the brown solution was cooled to room temperature, and water was added (50 mL) to induce precipitation. The crude product was filtered and purified by column chromatography ($\text{CHCl}_3/\text{MeOH}$ 9:1) to yield **9a** (35%), **4a** (16%), and **11a** (7%).

Reaction Conditions (d). The title compound was placed in a flask containing ethane-1,2-diamine (15 mL), and the mixture was stirred at rt for 16 h under argon. The resulting red mixture was poured in HCl (1 N, 100 mL). The solid orange solid was filtered and washed with water. Further purification by column chromatography (CHCl_3/Cy 6:4) gave pure **4a** (5% yield) and **10a** (72% yield).

***N,N'*-Dipentyl-naphthalene-1,4,5,8-tetracarboxylic Acid Bisimide (9a)**. Gray solid. ^1H NMR (300 MHz, CDCl_3 , 25 °C, TMS): δ 8.75 (s, 1H), 4.19 (t, J = 7.5 Hz, 4H), 1.75 (broad s, 4H), 1.42 (broad s, 8H), 0.96 (t, J = 6.0 Hz, 6H). ^{13}C NMR (300 MHz, CDCl_3 , 25 °C, TMS): δ 162.70; 133.01; 131.07; 130.79; 126.50; 40.83; 29.05; 27.62; 22.27; 13.84. MS (EI): m/z calcd for $\text{C}_{24}\text{H}_{26}\text{N}_2\text{O}_4$ 406.47, found 406.50. Anal. Calcd: C, 70.92; H, 6.45; N, 6.89; O, 15.74. Found: C, 70.95; H, 6.51; N, 6.82.

***N,N'*-Dipentyl-5,8,9,10-(1,4-diaza-1,2,3,4-tetrahydroanthracene)tetracarboxylic Acid Bisimide (4a)**. Yellow-gold solid. ^1H NMR (300 MHz, CDCl_3 , 25 °C, TMS): δ 10.60 (s, 2H), 8.25 (s, 2H), 4.15 (m, 4H), 3.80 (s, 4H), 1.70 (broad s, 4H), 1.45 (broad s, 8H), 0.95 (m, 6H). ^{13}C NMR (300 MHz, CDCl_3 , 25 °C, TMS): δ 166.27; 163.28; 143.72; 130.75; 126.25; 124.48; 122.2; 40.18; 38.07; 29.20; 27.63; 22.36; 13.89. MS (EI): m/z calcd for $\text{C}_{26}\text{H}_{30}\text{N}_4\text{O}_4$ 462.23, found 462.54. Anal. Calcd: C, 67.51; H, 6.54; N, 12.11; O, 13.84. Found: C, 67.42; H, 6.55; N, 12.32.

***N,N'*-Dipentyl-5,6,11,12-(1,4,7,10-tetraaza-1,2,3,4,7,8,9,10-octahydroanthracene)tetracarboxylic Acid Bisimide (11a)**. Violet solid. ^1H NMR (300 MHz, CDCl_3 , 25 °C, TMS): δ 10.79 (s, 4H), 4.15 (broad s, 4H), 3.73 (m, 8H), 1.73 (broad s, 4H), 1.43 (broad s, 8H), 0.94 (broad s, 6H). MS (EI): m/z calcd for $\text{C}_{28}\text{H}_{34}\text{N}_6\text{O}_4$ 518.61, found 519.70. Anal. Calcd: C, 64.85; H, 6.61; N, 16.20; O, 12.34. Found: C, 65.02; H, 6.65; N, 16.12.

General Thermal Procedure for the Synthesis of 12a and 13a According the Second Synthetic Protocol (See Scheme 3). To a stirred suspension of dibromodianhydride (600 mg, 0.001 mol) in glacial acetic acid (15 mL) was added pentylamine (1.6 mL). After being stirred for 30 min at 130 °C, the reaction mixture was cooled to room temperature and quenched into ice. The crude

orange solid was filtered on a Hirsch filter and purified by column chromatography (CH_2Cl_2), yielding **12a** (45%), **13a** (47%), and **12b** (11%).

***N,N'*-Dipentyl-2,6-dibromonaphthalene-1,4,5,8-tetracarboxylic Acid Bisimide (12a)**. Yellow solid. ^1H NMR (300 MHz, CDCl_3 , 25 °C, TMS): δ 9.02 (s, 2H), 4.21 (t, J = 7.6 Hz, 4H), 1.76 (broad s, 4H), 1.42 (broad s, 8H), 0.94 (t, J = 6.8 Hz, 6H). ^{13}C NMR (300 MHz, CDCl_3 , 25 °C, TMS): δ 160.63; 138.93; 128.19; 127.61; 125.25; 124.00; 41.45; 29.04; 27.45; 22.23; 13.81. MS (EI): m/z calcd for $\text{C}_{24}\text{H}_{24}\text{Br}_2\text{N}_2\text{O}_4$ 562.01, found 564.27. Anal. Calcd: C, 51.09; H, 4.29; Br, 28.32; N, 4.96; O, 11.34. Found: C, 51.01; H, 4.31; Br, 28.41; N, 5.02.

***N,N'*-Dicyclohexyl-2,6-dibromonaphthalene-1,4,5,8-tetracarboxylic Acid Bisimide (12b)**. Yellow solid. ^1H NMR (300 MHz, CDCl_3 , 25 °C, TMS): δ 8.7 (s, 2H), 5.09 (m, 2H), 2.63–2.48 (m, 4H), 1.93 (m, 4H), 1.75 (m, 6H), 1.45–1.27 (m, 6H). ^{13}C NMR (300 MHz, CDCl_3 , 25 °C, TMS): δ 163.19; 130.70; 126.79; 54.34; 29.59; 28.99; 26.37; 25.22. MS (EI): m/z calcd for $\text{C}_{26}\text{H}_{24}\text{Br}_2\text{N}_2\text{O}_4$ 588.22, found 588.31. Anal. Calcd: C, 53.08; H, 4.11; Br, 27.16; N, 4.76; O, 10.88. Found: C, 53.15; H, 4.10; Br, 27.21; N, 4.74.

***N,N'*-Dipentyl-2-bromonaphthalene-1,4,5,8-tetracarboxylic Acid Bisimide (13a)**. White solid. ^1H NMR (300 MHz, CDCl_3 , 25 °C, TMS): δ 8.96 (s, 1H), 8.81 (AB system, 2H), 4.20 (m, 4H), 1.76 (broad s, 4H), 1.43 (broad s, 8H), 0.94 (m, 6H). MS (EI): m/z calcd for $\text{C}_{24}\text{H}_{25}\text{BrN}_2\text{O}_4$ 485.37, found 486.45. Anal. Calcd: C, 59.39; H, 5.19; Br, 16.46; N, 5.77; O, 13.19. Found: C, 59.28; H, 5.15; Br, 16.42; N, 5.82.

***N,N'*-Dipentyl-2-(2'-aminoethylamino)-6-bromo-1,4,5,8-naphthalenetetracarboxylic Acid Bisimide (14a)**. Compound **12a** (200 mg, 0.35 mmol) was placed in a flask containing EDA (15 mL), and the mixture was stirred at rt for 2 h under argon. The resulting red mixture was washed with a solution of NaHCO_3 , and extracted, with CHCl_3 (3 \times 100 mL). The organic phases were combined, washed with water, and purified by column chromatography (CHCl_3) yielding **14a** as a red solid (50% yield). ^1H NMR (300 MHz, CDCl_3 , 25 °C, TMS): δ 10.31 (s, 1H), 8.82 (s, 1H), 8.26 (s, 1H), 4.19 (m, 4H), 3.66 (t, J = 5.8 Hz, 2H), 3.19 (t, J = 5.8 Hz, 2H), 1.74 (broad s, 4H), 1.42 (broad s, 8H), 0.94 (m, 6H). MS (EI): m/z calcd for $\text{C}_{26}\text{H}_{31}\text{BrN}_4\text{O}_4$ 543.45, found 543.52. Anal. Calcd: C, 57.46; H, 5.75; Br, 14.70; N, 10.31; O, 11.78. Found: C, 57.41; H, 5.76; Br, 14.71; N, 10.36.

Synthesis of **10a** and **10b** according synthetic procedure (d): The procedure (d), described above, was applied to compound **12a**. **12b** (0.35 mmol) yielding: **10a** (40%), **4a** (52%) and **10b** (33%), **4b** (60%), respectively.

***N,N'*-Dipentyl-6-bromo-5,8,9,10-(1,4-diaza-1,2,3,4-tetrahydroanthracene)tetracarboxylic Acid Bisimide (10a)**. ^1H NMR (300 MHz, CDCl_3 , 25 °C, TMS): δ 11.13 (s, 1H), 10.73 (s, 1H), 8.68 (s, 1H), 4.27 (m, 4H), 3.91 (s, 4H), 1.70 (broad s, 4H), 1.45 (broad s, 8H), 0.95 (m, 6H). ^{13}C NMR (300 MHz, CDCl_3 , 25 °C, TMS): δ 166.11; 165.55; 162.22; 161.30; 144.33; 143.36; 131.56; 125.04; 122.16; 121.41; 119.93; 40.69; 40.28; 38.16; 37.96; 29.26; 29.14; 27.57; 27.49; 22.36; 13.93; 13.89. MS (EI): m/z calcd for $\text{C}_{26}\text{H}_{29}\text{BrN}_4\text{O}_4$ 541.44, found 542.50. Anal. Calcd: C, 57.68; H, 5.40; Br, 14.76; N, 10.35; O, 11.82. Found: C, 57.42; H, 5.51; Br, 14.72; N, 10.28.

***N,N'*-Dicyclohexyl-6-bromo-5,8,9,10-(1,4-diaza-1,2,3,4-tetrahydroanthracene)tetracarboxylic Acid Bisimide (10b)**. Orange solid. ^1H NMR (300 MHz, CDCl_3 , 25 °C, TMS): δ 11.0 (s, 1H), 10.60 (s, 1H), 8.60 (s, 1H), 5.09 (m, 2H), 3.79 (s, 4H), 2.63–2.51 (m, 4H), 1.91 (m, 4H), 1.75 (m, 6H), 1.45–1.27 (m, 6H). MS (EI): m/z calcd for $\text{C}_{28}\text{H}_{29}\text{BrN}_4\text{O}_4$ 465.46, found 466.54. Anal. Calcd: C, 59.47; H, 5.17; Br, 14.13; N, 9.91; O, 11.32. Found: C, 59.41; H, 5.20; Br, 14.11; N, 10.01.

Mild Reductive Dehalogenation Yielding 4a (See Scheme 3). The reactant **10a** (0.07 mmol) was suspended in a solution of

34 mL of DMSO and 6 mL of water, degassed under nitrogen atmosphere, and stirred at room temperature. Sodium dithionite (0.6 mmol) was added, and the new mixture was stirred for 2 h at 40 °C. After this period, the reaction the excess of sodium dithionite was quenched by oxygen bubbling. After few minutes the precipitation of the product occurred. The resulting suspension was filtered and purified by column chromatography (CHCl₃/Cy 6:4) giving **4a** as a yellow solid (92%, yield).

***N,N'*-Dicyclohexyl-5,8,9,10-(1,4-diaza-1,2,3,4-tetrahydroanthracene)tetracarboxylic Acid Bisimide (4b)**. Yellow-gold solid. ¹H NMR (300 MHz, CDCl₃, 25 °C, TMS): δ 10.68 (s, 2H), 8.33 (s, 2H), 5.09 (m, 2H), 3.79 (s, 4H), 2.63–2.51 (m, 4H), 1.93 (m, 4H), 1.75 (m, 6H), 1.45–1.27 (m, 6H). ¹³C NMR (300 MHz, CDCl₃, 25 °C, TMS): δ 167.18; 163.95; 143.92; 124.71; 122.76; 122.40; 53.57; 38.14; 29.00; 26.51; 25.41. MS (EI): *m/z* calcd for C₂₈H₃₀N₄O₄ 486.56, found 486.23. Anal. Calcd: C, 69.12; H, 6.21; N, 11.51; O, 13.15. Found: C, 69.18; H, 6.26; N, 11.42.

2,7-*N,N'*-Dipentyltetraazabenzopyrene-1,3,6,8,10,11-hexaone (5a). The reactant **4a** (150 mg, 0.0003 mol) was dissolved in 30 mL of H₂O, 5 mL of concd H₂SO₄, and 5 mL of acetone. Then K₂Cr₂O₇ (200 mg, 0.0007 mol) was added to the solution. The brown mixture was heated at 100 °C for 1 h. After this period, the solution became clear, and then an other equal amount of K₂Cr₂O₇ was added and the solution was refluxed for other 2 h. The solution was cooled to room temperature, quenched in ice, neutralized with solid Na₂CO₃, and extracted with CHCl₃ (3 × 50 mL). The combined organic phases were washed with brine, and the solvent was removed under vacuum. The crude product collect was purified by column chromatography (CHCl₃) as a yellow solid or by preparative HPLC using CH₃CN/H₂O = 1:1 as eluent (yield: 75%). ¹H NMR (300 MHz, CDCl₃, 25 °C, TMS): δ 13.31 (s, 2H), 8.78 (s, 2H), 4.24 (m, 4H), 1.79 (broad s, 4H), 1.43 (broad s, 8H), 0.95 (m, 6H). ¹³C NMR (300 MHz, CDCl₃, 25 °C, TMS): δ 165.11; 161.80; 152.31; 132.82; 130.30; 125.50; 122.81; 105.94; 41.00; 29.00; 27.43; 22.22; 13.82. MS (EI): *m/z* calcd for C₂₆H₂₆N₄O₆ 490.51, found 491.6 (100.0), 463 (55.1), 393 (48.8), 323 (60.7). Anal. Calcd: C, 63.66; H, 5.34; N, 11.42; O, 19.57. Found: C, 63.62; H, 5.38; N, 11.58.

2,7-*N,N'*-Dicyclohexyltetraazabenzopyrene-1,3,6,8,10,11-hexaone (5b). Yellow solid. Yield: 64%. ¹H NMR (300 MHz, CDCl₃, 25 °C, TMS): δ 13.48 (s, 2H), 8.85 (s, 2H), 5.17 (m, 2H), 2.67–2.60 (m, 4H), 2.08–2.04 (m, 4H), 1.90–1.86 (m, 6H), 1.45–1.27 (m, 6H). ¹³C NMR (300 MHz, CDCl₃, 25 °C, TMS): δ 164.67; 164.14; 152.49; 132.82; 130.44; 125.50; 122.81; 105.94; 55.06; 29.71; 28.98; 26.45; 25.30. MS (EI): *m/z* calcd for C₂₈H₂₆N₄O₆ 514.53, found 515.54. Anal. Calcd: C, 65.36; H, 5.09; N, 10.89; O, 18.66. Found: C, 65.52; H, 5.02; N, 10.93.

Synthesis of 15a. Compound **5a** (0.030 g, 0.1 mmol) was dissolved in CHCl₃ (15 mL), and then a portion of CH₂N₂ (0.05 mmol; Et₂O 1 mL) was added to the stirred solution. The solution become yellow. Five milliliters MeOH was added after 5 min, and the solvent was evaporated under vacuum. The crude product was purified by reversed-phase column chromatography (CH₃CN/H₂O = 1.1, pH 4) as a yellow solid (yield: 69%). ¹H NMR (300 MHz, CDCl₃, 25 °C, TMS): δ 13.47 (s, 1H), 8.86 (d, *J* = 7.6; 2H), 8.80 (d, *J* = 7.6; 2H), 4.42 (s, 3H), 4.25 (m, 4H), 1.78 (broad s, 4H), 1.44 (broad s, 8H), 0.95 (m, 6H). MS (EI): *m/z* calcd for C₂₇H₂₈N₄O₆ 504.53, found 505.45. Anal. Calcd: C, 64.27; H, 5.59; N, 11.10; O, 19.03. Found: C, 64.55; H, 5.42; N, 11.18.

Synthesis of 16a. Compound **15a** (0.030 g, 0.1 mmol) was dissolved in CHCl₃ (15 mL) and then to the stirring solution was added a portion of CH₂N₂ (0.2 mmol; Et₂O 7 mL). After a few

minutes, an orange solid began to precipitate. After 10 min, the solid was filtered on a Hirsh filter (yield: 98%). ¹H NMR (300 MHz, CDCl₃, 25 °C, TMS): δ 8.87 (s, 2H), 4.46 (s, 6H), 4.27 (m, 4H), 1.78 (broad s, 4H), 1.44 (broad s, 8H), 0.95 (m, 6H). MS (EI): *m/z* calcd for C₂₈H₃₀N₄O₆ 518.56, found 519.7 (64), 504 (100), 490 (10). Anal. Calcd: C, 64.85; H, 5.83; N, 10.80; O, 18.51. Found: C, 64.94; H, 5.72; N, 10.72.

Computational Details. All calculations were carried out using the Gaussian 03²⁷ program package for gas phase and solvent optimization. All the geometric structures of NDIH, QXH, NDI⁻, QX⁻, and their water clusters NDIH 3H₂O, QXH 3H₂O, NDI⁻ 3H₂O, QX⁻ 3H₂O, including the four isomeric clusters A–D, were fully optimized in the gas phase and in water solution using the hybrid density functional method PBE0 with the 6-31+G(d,p) basis set. PBE0 functional (also referred to as PBE1PBE) is a combination of the exact exchange (25%) with the Perdew–Burke–Ernzerhof exchange (PBE1) and correlation functionals (PBE). It has been extensively used by Barone for predicting reactivity in aqueous solution using PCM solvation models.²⁵ The bulk solvent effects on the geometries and energies of the reactants were calculated via the self-consistent reaction field (SCRF) method using the PCM as implemented in the B.05 version of Gaussian 03. The cavity is composed by interlocking spheres centered on non-hydrogen atoms with radii obtained by the HF parametrization of Barone known as the united atom topological model (UAHF).²⁶ Such a model includes the nonelectrostatic terms (cavitation, dispersion, and repulsion energy) in addition to the classical electrostatic contribution.

Acknowledgment. Financial support from the Italian Ministry of University and Research (MIUR, FIRB-Ideas Project RBID082ATK_003) and the Italian Association for Cancer Research (Associazione Italiana per la Ricerca sul Cancro, or AIRC Grant No. 5826) is gratefully acknowledged. We are indebted to Dr. Lorenzo Mosca for helpful support with the p*K*_a measurements.

Supporting Information Available: UV/vis spectra of **5b**. ¹H NMR and ¹³C NMR for the NDIs: **4a,b**, **5a,b**, **6a–9a**, **10a,b**, **11a**, **12a,b**, and **–16a**. Cartesian coordinates, energies (in hartrees) and dipole moments (in debyes) for the structures NDIH, QXH, NDI⁻, QX⁻, and the water clusters NDIH 3H₂O, QXH 3H₂O, NDI⁻ 3H₂O, QX⁻ 3H₂O in the gas phase, and in water solution, at the PBE0/6-31+G(d,p) and PBE0-PCM/6-31+G(d,p) levels of theory. This material is available free of charge via the Internet at <http://pubs.acs.org>.

(27) *Gaussian 03, revision D.02*: Frisch, M. J.; Trucks, G. W.; Schlegel, H. B.; Scuseria, G. E.; Robb, M. A.; Cheeseman, J. R.; Montgomery, J. A., Jr.; Vreven, T.; Kudin, K. N.; Burant, J. C.; Millam, J. M.; Iyengar, S. S.; Tomasi, J.; Barone, V.; Mennucci, B.; Cossi, M.; Scalmani, G.; Rega, N.; Petersson, G. A.; Nakatsuji, H.; Hada, M.; Ehara, M.; Toyota, K.; Fukuda, R.; Hasegawa, J.; Ishida, M.; Nakajima, T.; Honda, Y.; Kitao, O.; Nakai, H.; Klene, M.; Li, X.; Knox, J. E.; Hratchian, H. P.; Cross, J. B.; Bakken, V.; Adamo, C.; Jaramillo, J.; Gomperts, R.; Stratmann, R. E.; Yazyev, O.; Austin, A. J.; Cammi, R.; Pomelli, C.; Ochterski, J. W.; Ayala, P. Y.; Morokuma, K.; Voth, G. A.; Salvador, P.; Dannenberg, J. J.; Zakrzewski, V. G.; Dapprich, S.; Daniels, A. D.; Strain, M. C.; Farkas, O.; Malick, D. K.; Rabuck, A. D.; Raghavachari, K.; Foresman, J. B.; Ortiz, J. V.; Cui, Q.; Baboul, A. G.; Clifford, S.; Cioslowski, J.; Stefanov, B. B.; Liu, G.; Liashenko, A.; Piskorz, P.; Komaromi, I.; Martin, R. L.; Fox, D. J.; Keith, T.; Al-Laham, M. A.; Peng, C. Y.; Nanayakkara, A.; Challacombe, M.; Gill, P. M. W.; Johnson, B.; Chen, W.; Wong, M. W.; Gonzalez, C.; Pople, J. A. Gaussian, Inc.: Wallingford, CT, 2004.